A new high-order fluid solver for tokamak edge plasma transport simulations based on a magnetic-field independent discretization

G Giorgiani, Thomas Camminady, Hugo Bufferand, Guido Ciraolo, Philippe Ghendrih, Hervé Guillard, Holger Heumann, B Nkonga, Frederic Schwander, Eric Serre, et al.

A new high-order fluid solver for tokamak edge plasma transport simulations based on a magnetic-field independent discretization

G. Giorgiani*,[1] T. Camminady,[2] H. Bufferand,[1] G. Ciraolo,[1] P. Ghendrih,[1] H. Guillard,[3] H. Heumann,[3] B. Nkonga,[3] F. Schwander,[4] E. Serre,[4] and P. Tamain[1]

[1]*IRFM, CEA Cadarache, F-13108 St. Paul-lez-Durance, France*
[2]*Department of Mathematics, CCES, 52062 Aachen, Germany*
[3]*INRIA Sophia Antipolis, 2004 Route de Lucioles, 06902 Valbonne, France*
[4]*Aix-Marseille Univ., CNRS, Centrale Marseille, M2P2 Marseille, France*

Correspondence: *G. Giorgiani, CEA-Cadarache, F-13108 St. Paul-lez-Durance, France. Email: giorgio.giorgiani@cea.fr

Summary

Our global understanding of the power exhaust in tokamaks, and its implications for both steady-state and transient heat loads on divertor and limiter PFCs, is still poor. In transient situations in particular, such as during start-up or control operations, the evolution of particles and heat fluxes is little known, although being critical for the safety of the machine.
The heat load is largely determined by the physics of the Scrape-Off Layer (SOL), and therefore it depends on a large extent on the geometry of the magnetic surfaces as well as on the geometry of wall components. A better characterization of the heat exhaust mechanisms requires therefore to improve the capabilities of the transport codes in terms of geometrical description of the wall components and in terms of the description of the magnetic geometry. For transient simulations, it also becomes crucial to be able to deal with non-stationary magnetic configurations. In particular, avoiding expensive re-meshing of the computational domain is mandatory.
As an attempt to achieve this goals we propose a new fluid solver based on a high-order hybrid discontinuous Galerkin (HDG) finite element method. Capitalizing on the experience acquired in the development of the SOLEDGE2D-EIRENE transport model, we propose to study the edge plasma transport in the frame of a reduced model (but containing most of the challenging issues regarding accurate numerical simulations) based on electron density and parallel momentum. The code is verified using manufactured solutions and validated using well-referenced simulations in a realistic WEST geometry. Finally, we show how the particle fluxes at the wall vary in our model when evolving the magnetic equilibrium in time, particularly during the equilibrium construction skipping from a limiter configuration to a diverted one at the beginning of the operation.

Keywords: Discontinuous Galerkin, Hybridization, Plasma physics, Tokamaks, Fusion

1 Introduction

The thermal power generated in the plasma core flows to the reactor wall through a narrow plasma boundary layer, called the Scrape-Off Layer (SOL), where the open magnetic field lines intercept the plasma facing components. The thickness of this boundary layer depends mainly on the ratio of the turbulent transport across magnetic field lines to the very rapid transport along them [6]. The dynamics of the plasma in this region plays a crucial role in the tokamak exhaust system, in the plasma re-fueling, and in the impurity dynamics.

Fluid models based on Braginskii equations, associated to Bohm boundary conditions at the plasma wall interface, remain standard in the international community to investigate turbulence and transport in the plasma edge under high-collisionality conditions (see [7]). Various 2D and 3D codes already exist, generally based on first and second-order finite-differences / finite-volumes numerical schemes (see a recent review of most of these codes in Refs. [9] and [3]). Two-dimensional transport codes solve axisymmetric averaged fluid equations in the plasma, while three-dimensional turbulent codes simulate self-consistently all scales of the flow (larger than the grid spacing). Despite the constant growth of the computational power, 3D codes remain computationally expensive. This will prevent performing routinely parametric studies to validate experimental scenarios in ITER. It remains thus clear today that engineering simulations in ITER size machines and in ITER relevant parameters will be only performed by 2D transport codes providing mean flow solutions.

[0]**Abbreviations:** PFC, plasma facing components; SOL, scrape-off layer; HDG, hybridizable discontinuous Galerkin; WEST, tungsten environment in steady-state tokamak

In this framework, progressing towards predictive simulations requires both to progressively enrich the physics included in the models and to continuously improve the accuracy and efficiency of the numerical schemes. To this aim, we explored the use of a high-order hybrid discontinuous Galerkin (HDG) finite-element method, that works on unstructured non-aligned discretizations. This new approach has been recently detailed in [4], where in particular, validation tests have shown the ability of the new solver to discretize accurately real geometries and to extend computations up to the tokamak center.

In this paper, we would like to explore another capability of the solver to deal with non-steady magnetic configurations, without requiring a very expensive on the fly remeshing of the computational domain. Although little studied till now, these non-steady magnetic configurations are critical for the safety of the tokamak during operation. Such a critical situation is the startup of the tokamak, during which the magnetic field evolves in few ms from limiter to divertor configuration. During this limiter/divertor transition, where the plasma wall interface moves from the tokamak first wall to the divertor target plates, the evolution of particles and heat fluxes is poorly known, although being critical for the safety of the machine. During fusion operation also, plasma control can require changing the plasma equilibrium by sweeping the strike points location in the tokamak chamber, in order to get a larger operating density range for partially detached plasmas with large radiative losses, or to better remove fusion ashes by increasing pumping for example. The paper is based on a reduced model of advection-diffusion equations for the ion density n and the particle flux Γ in the direction parallel to the magnetic field, Section 2. In Section 3 the main mathematical features of the HDG scheme are briefly described. In Section 4, simulations involving non-steady magnetic configurations are presented, corresponding to limiter/divertor transition during the start up of the machine.

2 Physical model

We consider the WEST geometry. The magnetic field $\mathbf{B}$ is prescribed at each time step, and encompasses both closed and open flux surfaces. The strong difference of intensity between the poloidal and toroidal components of the magnetic field ($\|\mathbf{B}_p\| << \|\mathbf{B}_t\|$) leads to a privileged flow direction along which the governing equations are projected using differential operators $\boldsymbol{\nabla}_\parallel = \boldsymbol{b}\cdot\boldsymbol{\nabla}$ and $\boldsymbol{\nabla}_\perp = \boldsymbol{\nabla} - \boldsymbol{b}\boldsymbol{\nabla}_\parallel$, where $\boldsymbol{b} = \frac{\mathbf{B}}{\|\mathbf{B}\|}$ is the unitary vector parallel to the magnetic field.

Two-dimensional fluid conservation equations for electrons and ions can be derived using simplified closures developed by Braginskii [1]. Under some hypothesis and ordering detailed in Refs. [9, 10], a minimum system involving the ion density n and parallel momentum $\Gamma = nu$ can be considered.

In the drift ordering hypothesis used in this work (see more details in [9, 10]), it is also useful to split the analysis of the dynamics into the parallel and perpendicular directions to the magnetic field, by decomposing the velocity vector $\boldsymbol{u}$ as

$$\boldsymbol{u} = u\boldsymbol{b} + \boldsymbol{u}_\perp, \tag{1}$$

where u is the component of the velocity parallel to the magnetic field. In this decomposition, the perpendicular component of the velocity is exact, and described in terms of drifts [9]. In this first stage of development, drifts are restricted for simplicity to the ion diamagnetic drift, which is substituted by a curvature drift velocity, $\boldsymbol{u}_{\nabla B}$, to account for the diamagnetic cancellation like in [9]:

$$\boldsymbol{u}_\perp = \boldsymbol{u}_{\nabla B} = \frac{2T}{B}(\boldsymbol{B}\times\boldsymbol{\nabla}B)/B^2,$$

where T is the temperature in eV, and having called B the magnetic field intensity, $B = \|\boldsymbol{B}\|$. This velocity represents the particle guiding center drifts in an inhomogeneous magnetic field.

Then, in the quasi-neutral limit ($n_e \approx Zn_i$) and neglecting the electron inertia ($m_e/m_i \simeq O(10^{-3})$), the system for an isothermal plasma writes in dimensionless form

$$\begin{cases} \partial_t n + \boldsymbol{\nabla}\cdot(\Gamma\boldsymbol{b} + n\boldsymbol{u}_\perp) - \boldsymbol{\nabla}\cdot(D\boldsymbol{\nabla}_\perp n) = S_n, \\ \partial_t\Gamma + \boldsymbol{\nabla}\cdot(\dfrac{\Gamma^2}{n}\boldsymbol{b} + \Gamma\boldsymbol{u}_\perp) + \boldsymbol{\nabla}_\parallel(c_s^2 n) - \boldsymbol{\nabla}\cdot(\mu\boldsymbol{\nabla}_\perp\Gamma) = S_\Gamma, \end{cases} \tag{2}$$

where the decomposition (1) is used. The sources S_n and S_Γ drive the particle and momentum flux, respectively, while the symbol c_s denotes the dimensionless sound speed. The effective diffusion coefficients D and μ take into account for both collisional transport and turbulence in the cross-field direction (described via a gradient diffusion hypothesis). They are assumed to be constant, and are usually chosen smaller than one. In the present paper they are also assumed to be equal, $D = \mu$. Please refer to Ref. [4] for details on the non-dimensionalization used to obtain this system.

Note that, in contrast to the physical model presented in [4], an extra term must be taken into account to deal with non-steady magnetic configurations. In fact, the time derivative of the plasma momentum now also accounts for the time variation of the vector $\boldsymbol{b}$. From the definition of Γ we have

$$\partial_t \Gamma = \partial_t (n\boldsymbol{u} \cdot \boldsymbol{b}) = \boldsymbol{b} \cdot \partial_t (n\boldsymbol{u}) + n\boldsymbol{u} \cdot \partial_t \boldsymbol{b} \approx \ \partial_t (nu) + n\boldsymbol{u} \cdot \partial_t \boldsymbol{b},$$

where the relations $\boldsymbol{b} \cdot \partial_t \boldsymbol{b} \equiv 0$ and $\boldsymbol{u}_\perp \cdot \boldsymbol{b} \equiv 0$ have been used, and the derivative of the drift velocity have been neglected, $\partial_t \boldsymbol{u}_\perp \approx 0$. This approximation relies on the hypothesis of slow varying magnetic field and the fact that the drift velocity $\boldsymbol{u}_\perp$ produces a small effect at the diffusion values considered in the numerical experiments, see also [4]. Hence, the term $n\boldsymbol{u} \cdot \partial_t \boldsymbol{b}$ is added to the formulation described in [4].

Boundary conditions. The system is supplemented with appropriate boundary conditions modeling the plasma-wall interaction. At the wall, the density is left free and the plasma-wall interaction is usually described in such a model by the Bohm boundary conditions for the parallel velocity [8]. That leads to impose an outgoing sonic/supersonic isothermal velocity at the wall such that:

$$\begin{aligned} \Gamma &\geq +n \quad \text{if } \boldsymbol{b} \cdot \boldsymbol{n} > 0, \\ \Gamma &\leq -n \quad \text{if } \boldsymbol{b} \cdot \boldsymbol{n} < 0, \end{aligned} \tag{3}$$

where $\mathbf{n}$ is the outer normal to the wall surface. However, when magnetic field lines are almost tangent to the wall ($|\boldsymbol{b} \cdot \boldsymbol{n}| \approx 0$), the Bohm theory fails. Hence, a threshold value t_h is defined in the present simulations ($|\boldsymbol{b} \cdot \boldsymbol{n}| < 0.1$ that corresponds to an angle larger than $85°$, above which both the density and the momentum are left free, and a homogeneous Neumann condition $\partial_\perp(.) = 0$ is imposed.

When the computational domain is restricted to the plasma edge, boundary conditions are also required to model the interaction with the core. Dimensionless boundary conditions can be both of Dirichlet type, with $n = 1$ and $\Gamma = 0$, or of Neumann type with $\partial_\perp(.) = 0$.

To conclude this section, let's remark that this reduced model contains most of numerical issues of more complete fluid edge models, i.e. the magnetic geometry complexity, the strong anisotropy between the directions parallel and perpendicular to the magnetic filed lines, as well as the wall description through Bohm boundary conditions.

3 The main mathematical feature of the new HDG scheme

A specific high-order HDG algorithm has been developed in this work to solve this 2D model in which the flow in the parallel direction corresponds to a compressible adiabatic gas flow, whereas in the perpendicular direction it corresponds to an incompressible flow, dominated by turbulence process. All details are provided in [4] and only the main mathematical features are introduced here.

The HDG scheme for the problem 2 consists in a two steps solve: at first, a *local problem* is solved in each element of the finite-element discretization. The local problem itself is, in each element, a weak formulation of 2 written in conservative form. It allows to express the discrete unknowns, that is, the conservative variables $\boldsymbol{U} = \{n, n\Gamma\}$ in the element nodes, in terms of another approximation of the solution, called the trace solution, which is defined on the element borders. The trace solution is referred as $\widehat{\boldsymbol{U}}$. The second step of the HDG solution consists in setting up a *global problem* which allows to solve for $\widehat{\boldsymbol{U}}$ in the whole mesh skeleton. The global problem derives from the imposition of the continuity of the fluxes, in weak form, across element borders. Once $\widehat{\boldsymbol{U}}$ is obtained, it is possible to recover the elemental solution $\boldsymbol{U}$ in each element as a local post-process. It is easy to see that the introduction of $\widehat{\boldsymbol{U}}$, defined only in the element boundaries, reduces the size of the linear system generated by the finite element discretization, in particular for high-order elements.

The time discretization is fully implicit, and performed using either a first order Backward Euler scheme, either a second order Gear scheme [1]. The non-linear terms are linearized using a classic Newton-Raphson method. A steady-state version of the code is also implemented, that solves (2) neglecting the time derivatives.

The code has been verified using the steady-state version and a manufactured solution. Results, that can be found in [4], show the recovery of theoretical convergence rates for all the polynomial degrees tested.

In Ref. [4], the code has been benchmarked in a realistic WEST geometry with respect to SOLEDGE2D solutions [2], which is nowadays a well-referenced transport code in the magnetic fusion international community. This benchmark has shown a very good agreement between the two codes, that makes us confident in the capability of this new solver to provide reliable solutions in a complex realistic geometry.

[1] In the Gear scheme the time derivative is approximated as $df/dt|^{n+1} \approx 3/2 f^{n+1} - 2f^n + 1/2 f^{n-1}$

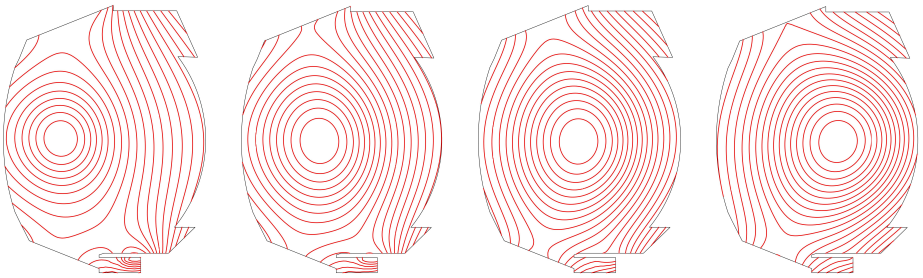

Figure 1: Evolving equilibrium: iso-contours of the magnetic flux at four snapshots of the magnetic configuration.

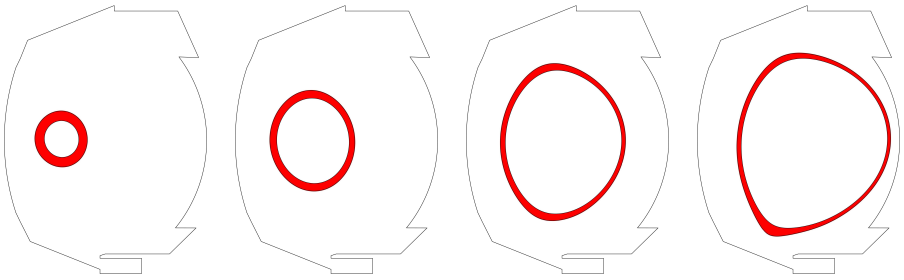

Figure 2: Evolving equilibrium: density source at four snapshots of the magnetic configuration.

4 WEST simulations of a limiter-divertor magnetic transition

One of the major assets of the non-aligned discretization is the possibility of computing the transport during an equilibrium evolution without the need of re-defining the computational mesh. Hence, the goal of this last numerical test is to show the capabilities of the code to deal with evolving magnetic fields. To this aim, the transition from limiter to divertor configuration in the WEST machine is considered. This is a typical operation which is performed at the startup of the machine.

The evolution of the magnetic fields during this transition is computed using the code FEEQS.M [2] that implements the methods described in [5]. In these simulations the free-boundary axisymmetric plasma equilibrium equations for the magnetic flux are augmented by circuit and induction equations due to the poloidal field coils and passive structures. The transition is mainly driven by externally applied time varying voltage sources. The evolution of the magnetic flux results itself in a perturbation of the toroidal component of the magnetic field. This perturbation is small compared to the toroidal field that is imposed by the toroidal field system. For this specific example the externally generated background field amounts to 3.6T at R= 3.5m and then, during the simulation, the total toroidal field evolves at the magnetic axis from 3.5T to 4.1T.

The global transition time is 45ms. A set of ten equilibria is saved, spaced by $dt = 5$ms, and used to perform the HDG transport simulation. In Figure 1 are shown four configurations of the magnetic flux at times $0, 15, 30, 45$ ms.

The set-up of the HDG transport simulation is as follows. A triangular mesh consisting of 35132 $p = 3$ elements is used, and the first-order time integration scheme is selected. The physical parameters are : $T_0 = 50$eV, $D = \mu = 0.038$ $(= 1m^2s^{-1})$. A steady-state solution is at first computed using the first magnetic field configuration (at $t = 0s$), imposing a source of density (at zeros velocity) of constant intensity, located in the region of space delimitated by two iso-lines of the magnetic flux. The integral of the source is equal to 1 in non-dimensional units. Starting from this initial steady-state solution, a moving equilibrium simulation consists in running a transient simulation in which, at each time step, a new magnetic configuration is loaded, and the non-linear solver is used to compute the time iteration. Since only 10 states were provided by FEEQS.M, additional equilibrium states were computed using a linear interpolation between two adjacent original states, if the required time step for the transient simulation were smaller than 5ms. In this preliminary tests, we chose to move the density source accordingly to the magnetic fields. This means that, during the transient simulation, at each time step the density source location is defined by the two iso-lines used to compute the starting steady-state condition. For this reason, the two values of the magnetic flux defining the two iso-lines are chosen to have a source that never touches the wall of the tokamak. In Figure 2 is shown the area of the density source for the first and the last magnetic configuration. The integral is kept constant during the whole simulation.

[2] http://www-sop.inria.fr/members/Holger.Heumann/Software.html

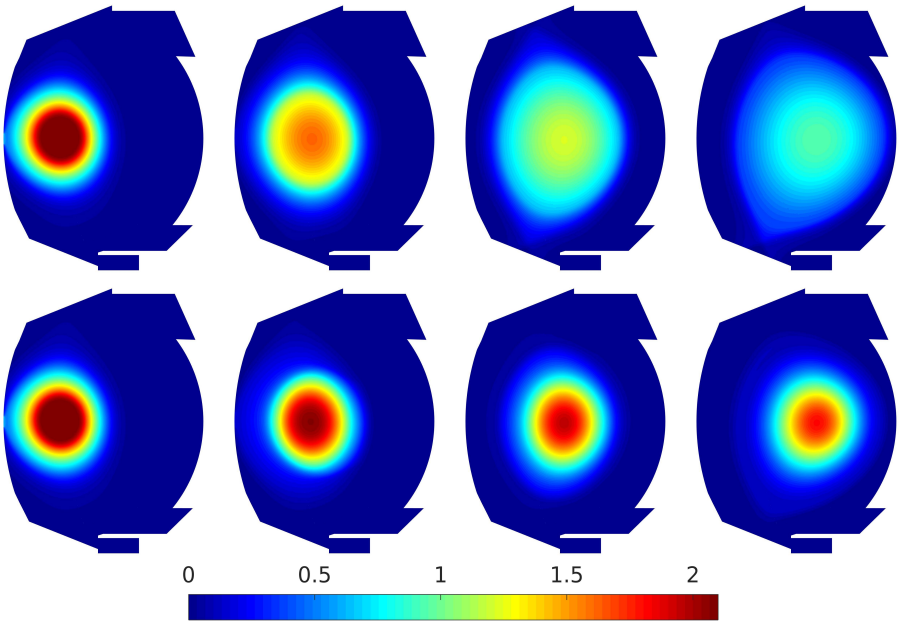

Figure 3: Evolving equilibrium: comparison between the map of the density n in the normal transition simulation (upper) and fast transition simulation (lower).

In order to study the response of the plasma to the transition speed, two different simulations were performed: in the first simulation, the transition takes 45ms, that is the time provided by the equilibrium code. We will refer to this case as the "normal" simulation. In the second simulation, the transition takes 4.5ms: this means that the ten equilibrium states provided by FEEQS.M are used to artificially produce a transition that is ten times faster than the one actually simulated. We will refer to this case as the "fast" simulation. In both cases, ten additional states were interpolated between each of the original magnetic states, resulting in a time step $dt = 0.5$ms for the normal simulation and $dt = 0.05$ms for the fast simulation.

The results are shown in Figures 3 and 4 for the times $t = [0, 30, 60, 90] \times dt$, for the normal (upper line) and fast (lower line) simulation. In Figure 3 is depicted the density n: in both simulations the plasma core follows the magnetic fields, but while in the normal simulation the density profile spreads out in the transition, in the fast simulation the perpendicular dynamics of the plasma is not fast enough to drive the density across the magnetic surfaces. As a consequence, the plasma core remains concentrated close to the magnetic axis. The parallel Mach profile during the transition is presented in Figure 4, where we observe the generation of two supersonic fronts in the fast simulation.

Figure 5 shows the outgoing flux of density in the lower divertor, the left limiter and the upper divertor. It can be noticed how, during the transition, the density flux passes gradually from the left limiter to the upper and lower divertors, both in the normal and fast simulation. In the normal simulation, the flux involves the lower and upper divertors around halfway the transition, but then the flux leaves the lower divertor. A strong outgoing flux is eventually established only in the lower divertor near the end of the simulation. In the fast simulation however, as stated earlier, the perpendicular dynamics is too slow to establish a steady-state outgoing flux. Indeed, there is almost no outgoing flux in the last configuration.

The two computations are then extended beyond the end of the transition. The final magnetic configuration is left fixed and the transport simulation is evolved until a steady-state condition is reached in both cases. The results in terms of outgoing flux are presented in Figure 6, for a computation time reaching 0.35s. As expected the two simulations reach the same steady-state represented by an outgoing flux of density involving only the lower divertor. It can be noticed how, in the fast simulation, the upper divertor is almost uncharged during the whole transition.

5 Conclusions

A new discontinuous Galerkin solver has been presented for solving 2D fluid transport equations in the plasma edge of a tokamak including both open and closed magnetic field lines. Associated to a finite elements discretization based on an unstructured mesh not aligned on the magnetic field, it also allows to accurately discretize any realistic tokamak chamber as well as any magnetic geometry. The high-order accuracy of the numerical scheme guarantees a low numerical diffusivity despite a discretization

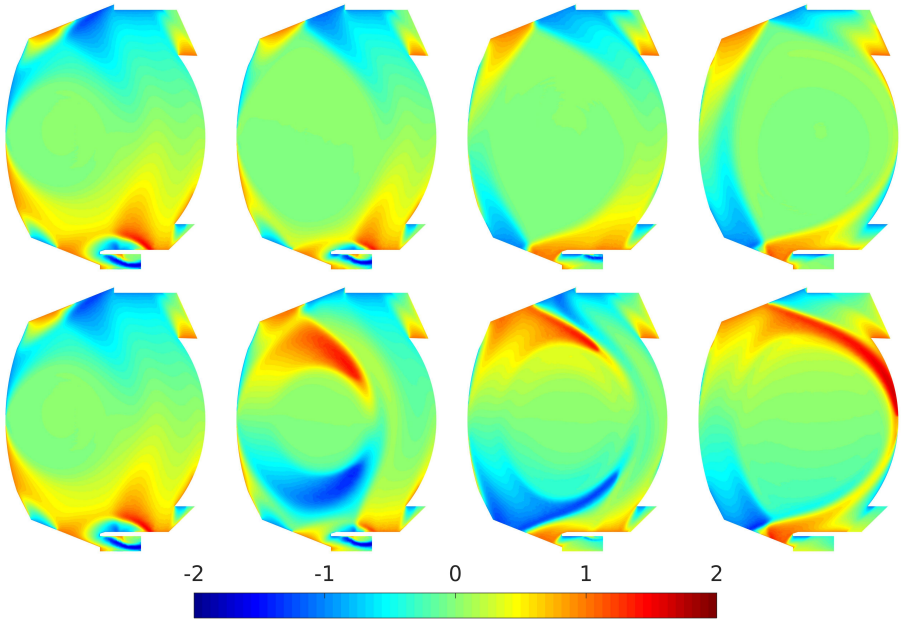

Figure 4: Evolving equilibrium: comparison between the map of the Mach number in the normal transition simulation (upper) and fast transition simulation (lower).

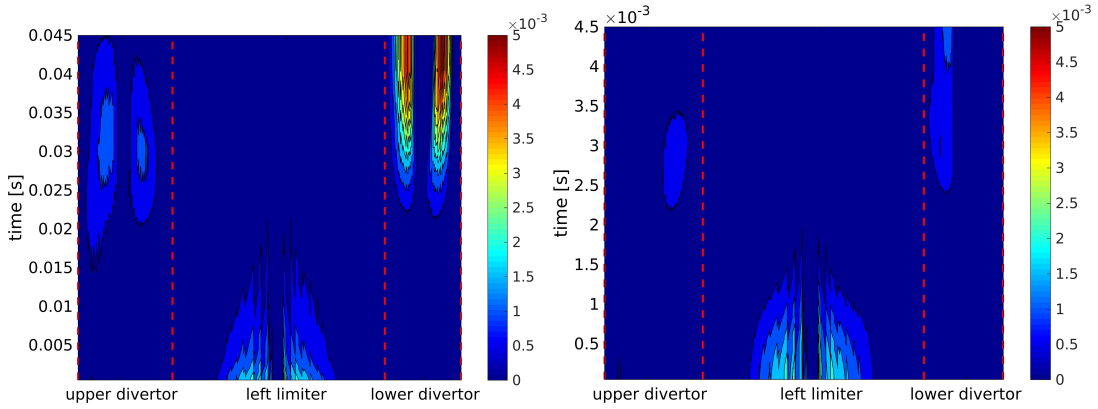

Figure 5: Evolving equilibrium: distribution of the outgoing flux of particles as a function of the time, in the slow transition simulation (left) and the fast transition simulation (right).

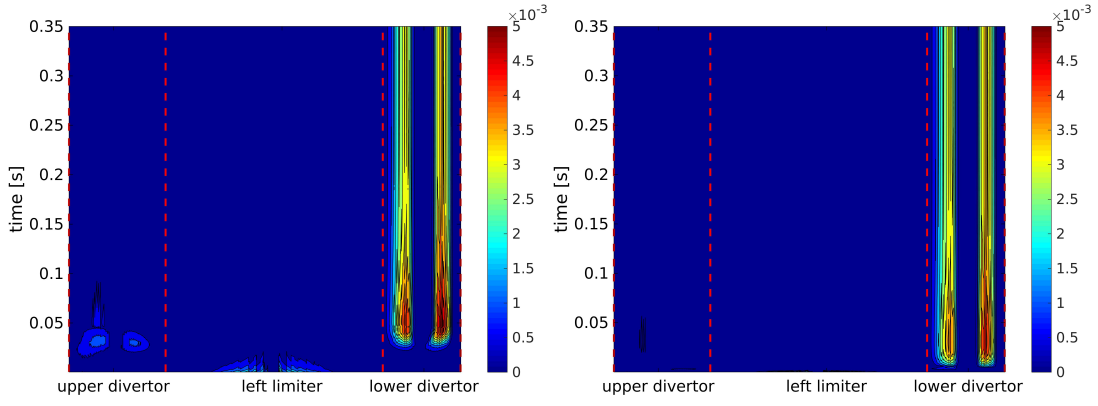

Figure 6: Evolving equilibrium: distribution of the outgoing flux of particles as a function of the time, in the slow transition simulation (upper) and the fast transition simulation (lower). Extended simulation in time with a final constant magnetic equilibrium.

of the differential operators not aligned on the magnetic field. This allows to consider non-stationary magnetic configurations that would require, with numerical methods usually implemented in transport codes, a very expensive on the fly re-meshing of the computational domain. This offers thus a flexibility on the magnetic configuration which is not available with classical structured meshes approaches based on finite-differences (volumes).

At this early stage, the solver is proposed on a reduced electrostatic model for the ion density and the parallel momentum, that however contains most of the numerical issues met in more complete fluid edge models, i.e. the magnetic geometry complexity, the strong anisotropy between the two magnetic filed lines directions, as well as the wall description through Bohm boundary conditions.

Verification and validation tests detailed in [4] have shown the expected $p+1$ rates of convergence during the h-refinement tests, as well as a good agreement with solutions of reference performed with the well-referenced transport code SOLEDGE2D in WEST tokamak.

First results with a non-steady magnetic configuration during a limiter/divertor transition in WEST illustrate the strong potential of this new solver to investigate heat exhaust physics during these transient states in the machine. This is a completely new feature in the landscape of nowadays codes for plasma transport simulations, and opens the path to new analysis including consistent simulations transport-equilibrium.

Acknowledgement

This work was granted access to the HPC resources of IDRIS under the allocation i2017056912 and i20170242 made by GENCI, and of Aix-Marseille University, financed by the project (ANR-10-EQPX-29-01). This work was supported by the Energy oriented Centre of Excellence (EoCoE), grant agreement number 676629, funded within the Horizon2020 framework of the European Union.

References

[1] S. I. Braginskii, *Reviews in Plasma Physics* **1965**, *1*, 205–311.

[2] H. Bufferand, B. Bensiali, J. Bucalossi, G. Ciraolo, P. Genesio, Ph. Ghendrih, Y. Marandet, A. Paredes, F. Schwander, E. Serre, P. Tamain, *J. Nucl. Mat.* **2013**, *84*, 445–448.

[3] H. Bufferand, G. Ciraolo, Y. Marandet, J. Bucalossi, Ph. Ghendrih, J. Gunn, N. Mellet, P. Tamain, R. Leybros, N. Fedorczak, F. Schwander, E. Serre, *Nucl. Fusion* **2015**, *55(5)*, 053025.

[4] G. Giorgiani, H. Bufferand, G. Ciraolo, P. Ghendrih, F. Schwander, E. Serre, P. Tamain, *J. Comp. Phys.* submitted.

[5] H. Heumann, J. Blum, C. Boulbe, B. Faugeras, G. Selig, J.-M. Ané, S. Brémond, V. Grandgirard, P. Hertout, E. Nardon, *J. Plasma Phys.* **2015**, *81(3)*.

[6] T. D. Rognlien, *Plasma Phys. Control. Fusion* **2005**, *47*, 283–295.

[7] B. Scott, *Phys. Plasmas* **2005**, *12*, 102307.

[8] P. C. Stangeby, *The plasma boundary of magnetic fusion devices* IOP (ed). **2000**.

[9] P. Tamain, H. Bufferand, G. Ciraolo, C. Colin, D. Galassi, Ph. Ghendrih, F. Schwander, E. Serre, *J. Comp. Phys.* **2016**, *321*, 606–623.

[10] P. Tamain, Ph. Ghendrih, E. Tsitrone, V. Grandgirard, X. Garbet, Y. Sarazin, E. Serre, G. Ciraolo, G. Chiavassa, *J. Comp. Phys.* **2009**, *229*, 361–378.